Journal of Orthopaedic Translation (2017) 8, 40—48

Available online at www.sciencedirect.com

ScienceDirect

journal homepage: http://ees.elsevier.com/jot

ORIGINAL ARTICLE

Bone cement allocation analysis in artificial cancellous bone structures

Ivan Zderic [a,*], Philipp Steinmetz [a], Lorin M. Benneker [b], Christoph Sprecher [a], Oliver Röhrle [c], Markus Windolf [a], Andreas Boger [d], Boyko Gueorguiev [a]

[a] *AO Research Institute Davos, Davos, Switzerland*
[b] *Department of Orthopedic Surgery, Inselspital, Berne University Hospital and University of Berne, Berne, Switzerland*
[c] *Institute of Applied Mechanics and Stuttgart Research Centre for Simulation Technology, Stuttgart, Germany*
[d] *Faculty of Engineering Sciences, Ansbach University of Applied Sciences, Ansbach, Germany*

Received 7 July 2016; received in revised form 19 August 2016; accepted 13 September 2016
Available online 4 October 2016

KEYWORDS
bone cement leakage;
flow behaviour;
foam model;
preoperative planning;
vertebroplasty

Summary *Background:* One of the most serious adverse events potentially occurring during vertebroplasty is cement leakage. Associated risks for the patient could be reduced if cement filling is preoperatively planned. This requires a better understanding of cement flow behaviour. Therefore, the aim of the present study was to investigate bone cement distribution in artificial inhomogeneous cancellous bone structures during a simulated stepwise injection procedure.

Methods: Four differently coloured 1-mL cement portions were injected stepwise into six open-porous aluminum foam models with simulated leakage paths. Each model was subsequently cross-sectioned and high-resolution pictures were taken, followed by anatomical site allocation based on the assumption about a posterior insertion of the cannula. A radial grid consisting of 36 equidistant beams (0°—350°) was applied to evaluate the cement flow along each beam by measuring the radial length of each cement portion (total length) and of all four portions together (distance to border). Independently from the injection measurements, the viscosity of 20 cement portions was measured at time points corresponding to the start of the first and the end of the last injection.

Results: Despite some diffuse colour transitions at the borderlines, no interfusion between the differently coloured cement portions was observed. The two highest values for total length of each of the first three injected cement portions and for distance to border were indicated in directions anterior bilateral to the cannula along the 120°, 240° and 250° beams and posterolateral along the 60° beam. The two highest total lengths for the fourth cement portion were registered in the direction of the cannula along the 170° and 180° beams. Standard deviations

* Corresponding author. Clavadelerstrasse 8, 7270 Davos Platz, Switzerland.
E-mail address: ivan.zderic@aofoundation.org (I. Zderic).

http://dx.doi.org/10.1016/j.jot.2016.09.002

of total length for each of the last three injected portions and for distance to border were with two highest values in directions anterior bilateral to the cannula along the 120°, 150°, 240° and 250° beams and opposite to the direction of the cannula along the 10° beam. The two highest values for the first cement portion were registered posterior bilateral to the cannula along the 70° and 350° beams. The values for averaged standard deviations of the total length of the fourth cement portion and the distance to border were significantly higher in comparison to the first cement portion ($p \leq 0.020$). Dynamic viscosity at the start of the first injection was 343 ± 108 Pa·s and increased to 659 ± 208 Pa·s at the end of the fourth injection.

Conclusion: The simulated leakage path seemed to be the most important adverse injection factor influencing the uniformity of cement distribution. Another adverse factor causing dispersion of this distribution was represented by the simulated bone marrow. However, the rather uniform distribution of the totally injected cement amount, considered as one unit, could be ascribed to the medium viscosity of the used cement. Finally, with its short waiting time of 45 s, the stepwise injection procedure was shown to be ineffective in preventing cement leakage.

Introduction

Osteoporotic fractures of vertebral bodies deform spine, cause chronic pain, impede patients' activities and limit their freedom of movement [1]. Vertebroplasty is currently a worldwide applied treatment procedure for bone cement augmentation in spine [2] with the main goal to restore mechanical strength and stiffness of the respective vertebral body. Several clinical studies reported an instant pain relief within 24 hours following treatment in 80—97% of the cases [3—5]. Despite all advantages, enhancing the mechanical competence is accompanied with increased risks of adjacent vertebral fractures [6,7]. The main complication in vertebroplasty is linked to cement leakage during the injection procedure, reported in 30—67% of the cases [8,9]. As the injection process is usually interrupted when leakage is noticed, the latter compromises the mechanical competence of the vertebral body because of insufficient cement filling. Additionally, the bone cement leaks into the surrounding tissue or draining veins, which can lead to pulmonary or fat embolism and nerve root or spinal cord compression, respectively [8,10].

Apart from existing approaches such as lavage technique [11,12], the use of high-viscosity cements [10,13] and directionally controlled side-opening cannulas [14], the risks of cement leakage could be further reduced by preoperative in silico planning of the cement filling process. Based on patient radiological data, a predefined cement volume and an ideal positioning of the cannulas could be determined. Therefore, in silico simulations are necessary to calculate the flow behaviour of the bone cement in the cancellous bone tissue. A twofold benefit would be achieved by preoperative planning: the risk of cement leakage could be minimised, and the mechanical properties of an augmented vertebra could be optimised.

However, preoperative planning of vertebroplasty would only make sense if it is ensured that bone cement spreads uniformly when parameters of the injection process are not changed. Baroud et al [10] and Boger and Wheeler [13] have shown that cement viscosity plays a crucial role in cement distribution in the cancellous bone tissues. The higher the viscosity, the more uniformly bone cement spreads and the lower the risk of cement leakage. The viscosity of bone cement increases during exothermic curing [15]. An increase in the viscosity requires increase in the applied injection forces [16]. An increase in the ambient temperature, e.g., while injecting the bone cement into the patient (37°C) results in a faster curing [15]. Moreover, Basafa et al [17] addressed the flow of bone cement in cancellous bone and created a validated model, which matched with the experimentally generated spread of bone cement (average, 86%). Based on the Theory of Porous Media, Bleiler et al [18] have proposed a validated multiphasic numerical model allowing to predict the cement distribution in a vertebral body.

Generally, the vertebroplasty procedure is performed stepwise. To the best of our knowledge, the interaction between subsequently injected cement portions and their distribution have not been investigated yet. In view of preoperative planning, future simulations should have to consider this stepwise injection process to create more realistic models. However, these models will be difficult to validate without understanding the interaction and distribution of different cement portions.

Therefore, the aim of the present study was to investigate bone cement distribution in open porous artificial inhomogeneous cancellous bone structures during a simulated stepwise vertebroplasty procedure.

Materials and methods

Specimens and preparation

Six specimens, S1—S6, consisting of laboratory cylindrical open-porous aluminum foam models (ERC Aluminum and Aerospace, CA, USA) with a diameter and height of 38.1 mm and 25.4 mm, respectively, porosity of 91.1 ± 0.6%

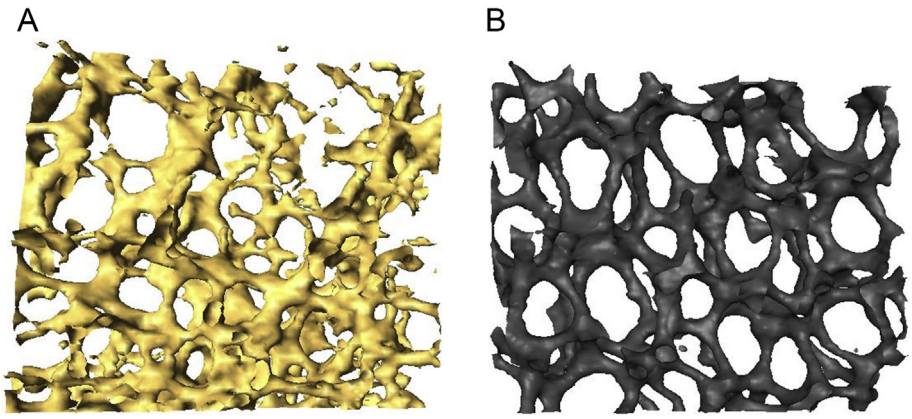

Figure 1 (A) Computed tomography image of a human osteoporotic cancellous bone; (B) computed tomography image of an open-porous aluminum foam model.

[mean ± standard deviation (SD)] and permeability of $8.47 \pm 0.26 \times 10^{-8}$ m^2 were used as validated substitutes for cancellous bone of osteoporotic thoracolumbar vertebral bodies [10]. The similarity in their pore size and cavity interconnection to human cadaveric cancellous bone is shown in Figure 1. The models contained a drilled leakage path measuring 3 mm in diameter in the main plane at a distance of 8 mm to the centre, mimicking an intravertebral blood vessel. A cylindrical channel, measuring 4.1 mm in diameter, was drilled up to the centre of the circular cross section radially and perpendicular to the leakage path in the main plane for cannula insertion. The foam models were filled with a water—cornstarch mixture as described in Boger and Wheeler [13] to substitute the bone marrow. They were further coated with 2-mm two-component acrylic cast resin (SCS-Beracryl D 28 Powder and SCS-Beracryl Liquid, Suter Kunststoffe AG, swiss-composite, Fraubrunnen, Switzerland) in order to simulate bone cortex.

Cement preparation

Bone cement with the composition described by Deusser et al [15] was used to prepare a total of four differently coloured cement portions, namely blue, red, yellow and green. After mixing, this cement is applicable within 20 ± 1 minutes at an ambient temperature of 18—26°C. It completely cures after 27 ± 2 minutes [15]. All cement portions were prepared at a total volume of 10 mL by applying a uniform manual mixing procedure under the same conditions. A 5-mg acrylic powder (Kremer Pigmente GmbH & Co KG, Aichstetten, Germany) was used for colouration. The powder was utilized in the intense colours red (#23180), yellow (#23310) and blue (#23050). In addition, green acrylic powder was assembled by mixing yellow and blue powders at a 10:1 mixture ratio. The powder and the liquid component of all cement portions assigned to one specimen were then simultaneously mixed in a separate beaker for 20 seconds, assuring the same start time of polymerization for all portions. After preparation, the blue-coloured bone cement was filled in a 2-mL syringe, whereas the other bone cement portions were filled in 1-mL syringes (Vertecem V+ Syringe Kit, DePuy Synthes, Zuchwil, Switzerland).

Test setup

An electromechanical test system (Instron 5866, Norwood, MA, USA), equipped with a 1-kN load cell was used for vertical cement injections into the foam models with a test setup shown in Figure 2. The prefilled 1-mL and 2-mL syringes, containing the coloured cement portions, were attached via Luer taper to the proximal end of 8-gauge

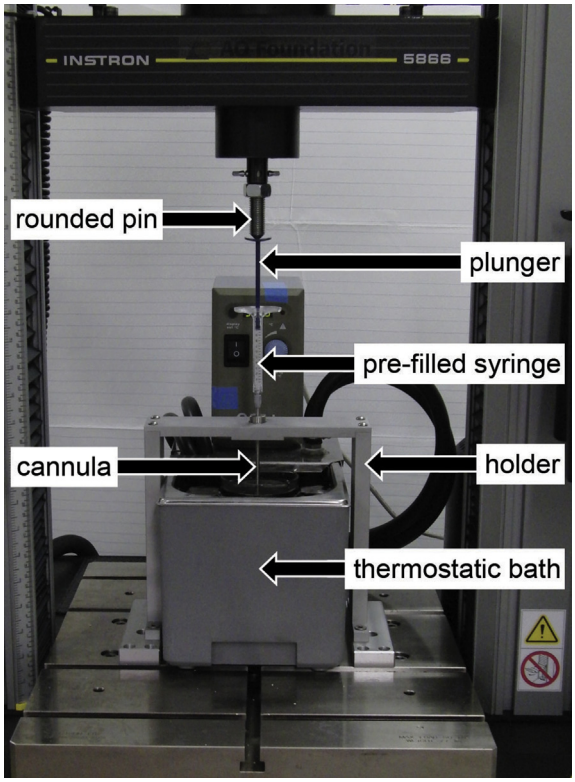

Figure 2 Test setup with pre-filled 1 ml-syringe mounted for injection. Reprinted from Medical Engineering & Physics, http://dx.doi.org/10.1016/j.medengphy.2016.09.015 [Epub ahead of print], Zderic I, Steinmetz P, Windolf M, Richards RG, Boger A, Gueorguiev B, Bone cement flow analysis by stepwise injection through medical cannulas, Copyright (2016), with permission from Elsevier.

medical cannulas (length = 150 mm; Unimed S.A., Lausanne, Switzerland). Vertical injection direction was assured by the insertion of the cannula through a custom-made holder. The distal end of the cannula was immersed 90 mm into a water-filled glass cylinder, which itself was inlaid in a water bath warmed up to 37°C (Y6, Grant Instruments Cambridge Ltd, Shepreth, UK). Thus, leaking bone cement was kept in the glass cylinder. A rounded, headless pin was attached to the load cell enabling load transmission centrally on the plungers of the syringes. Prior to the start of the experiment, each foam model was packed in individually labelled plastic bags and warmed up in another water bath at 37°C. For the injection, the models were taken individually out of the water bath and placed into the custom-made holder placed at the bottom of the glass cylinder, allowing proper orientation of the drilled hole for the vertical cannula insertion. Being fastened by the holder, the distal end of the cannula was then inserted into the foam model.

Test protocol

The four differently coloured bone cement portions were injected in four subsequent steps in the following order: green, red, yellow and blue. After each injection, the used syringe was replaced by the next one. A constant flow rate of 7.0 mL/min was set for the first three injections in each specimen according to Baroud et al [10]. For injecting exactly 1.0 mL of cement, the piston had to cover a distance of 54 mm through the route of the 1-mL syringe. Consequently, the machine transducer was set to act with a constant speed of 378.1 mm/min on the syringe plunger. Same protocol was used for the injection of the fourth blue cement portion with a 2-mL syringe, thereby injecting a total volume of 1.79 mL. As a result, the respective injected volume in the foam was 0.73 mL due to the remaining amount in the cannula after the final injection step.

Prior to and after injection, each foam model was scanned using high-resolution peripheral quantitative computed tomography (CT) (XtremeCT, Scanco Medical, Brüttisellen, Switzerland) at 82 μm nominal isotropic resolution, 60 kVp effective energy, 900 μA current and an integration time of 400 ms.

Independently from the injection experiments, the viscosity of 20 additionally prepared cement portions was measured using a rheometer (Viscosafe Viscometer, DePuy Synthes, Switzerland). The measurements were started immediately after each portion had been mixed.

Postprocessing

Following the second scan, each foam model was cut in two sections through its middle plane, defined by both injection canal and leakage path, using a 0.3-mm-thick band saw. One sectioned specimen of each cut foam model was then selected for further analysis. High-resolution images of the six selected sections were taken under a macroscope (AxioCam HRc; Carl Zeiss Microscopy GmbH, Jena, Germany) with the aid of special software (AxioVision 4.8.2, Carl Zeiss Microscopy GmbH, Jena, Germany) at a pixel size of 5.771×10^{-2} mm^2.

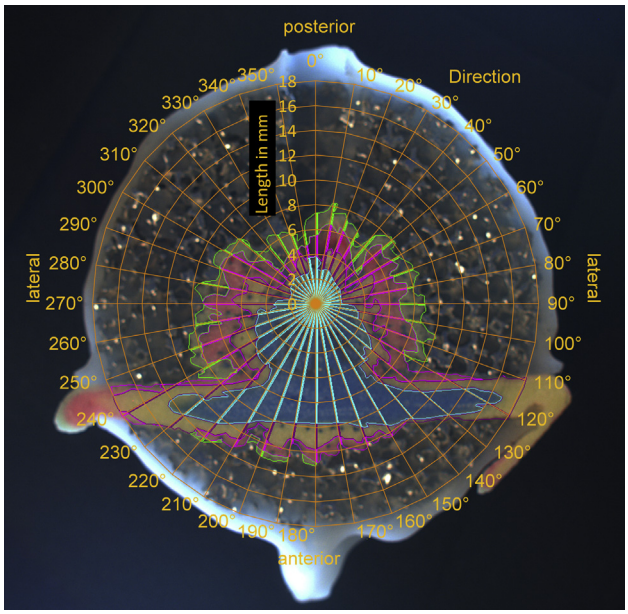

Figure 3 Macroscopic image of a sectioned specimen with applied 10° beam radial grid with totally 36 beams, and coloured sections of each beam according to the underlying cement portion.

First, the cross-sections were located according to the anatomical sites, posterior (0° beam), anterior (180° beam) and lateral (90° and 270° beams), as shown in Figure 3. To analyze the bone cement distribution, a radial grid was introduced upon the macroscopic images to directionally orientate the sections. Therefore, the midline of the drill hole for cannula insertion was overlaid with a beam originating in the centre of the circular section. This beam was defined as the 0° beam and was the base of the circle closing radial grid consisting of totally 36 beams, all originating from the centre. The inclination between two adjacent beams was 10°, revealing values in a range between 0° and 350°, which were assigned clockwise in ascending order to the respective beams. Each beam was further sectioned in accordance with the underlying transition of one cement portion to another.

Data acquisition and evaluation

The length of each section lying on each beam was calculated using image analysis software (KS 400 3.0, Carl Zeiss Microscopy GmbH, Jena, Deutschland). To quantify the directional flow, the total length of each cement portion was derived by adding up the length of the sections associated with the same cement portion and respective beam. Considering all four cement portions as one unit, the distance to the outer cement border along each beam was calculated by summing up the total length values of each single portion. This calculated distance actually represented and was equal to the distance from the centre of the circular section to the outer cement border along the respective beam. SD of each cement portion's averaged total length and distance to outer border values were determined and further separately

averaged over the 36 beams. Furthermore, beams characterised by the highest total length and distance to border values, as well as by the highest respective SDs, were determined. Finally, the surface area of each differently coloured cement portion was calculated based on the images of the sectioned specimens.

Preinjection and postinjection scans were used to calculate the intersection volume of the totally injected cement unit in the six specimens using the Simpleware ScanIP image processing software (Simpleware Ltd, Bradninch Hall, Great Britain) as follows: (1) first, the outer shell of the injected cement of each specimen was processed from its postinjection scan; (2) second, each of the six shells was virtually inserted into a properly oriented preinjection scan of one specimen; (3) third, the common region of the six overlapped shells was segmented, and the respective volume was calculated; and (4) finally, the fraction volume of the aluminum foam inside this common region was calculated and subtracted from its volume.

Viscosity measurements included recording of time after the start of polymerization and dynamic viscosity η at a rate of 1.3 Hz. The dynamic viscosity was evaluated 180 seconds and 330 seconds after the cement mixing, corresponding to the respective time window between the start of the first injection and the accomplishment of the fourth injection.

Statistical evaluation upon the parameters of interest was performed using the software package IBM SPSS (IBM SPSS Statistics Version 21, IBM Corporation, Armonk, NY, USA). Normal distribution and homogeneity of variance were checked using Shapiro—Wilk and Levene tests, respectively. Mann—Whitney test with Bonferroni *post hoc* correction was performed to screen the outcomes total length and distance to border for significant differences between the differently coloured cement portions. A one-way analysis of variance (ANOVA) with Games—Howell *post hoc* test was conducted to detect significant differences between the surface areas of these portions. The level of significance was set to 0.05 for all statistical tests.

Results

The sectional images of the foam models showed, apart from the leakage paths, a relatively circular cement

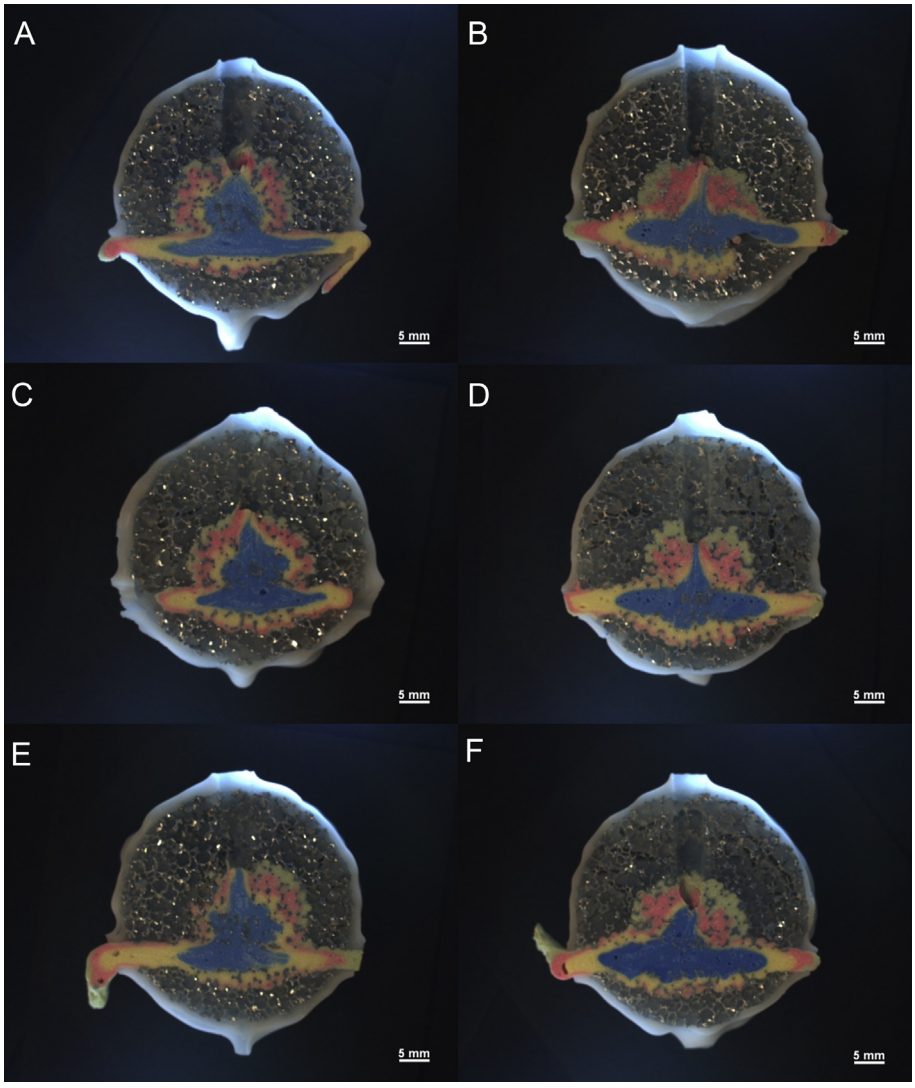

Figure 4 (A—F) Visual representation of one section through the middle plane of each specimen S1—S6.

pattern with distinct borderlines between the cement portions. Despite some diffuse colour transitions at the borderlines, no interfusion of the differently coloured bone cement portions was observed. The section of each specimen selected for analysis is shown in Figures 4A–4F. Bone cement bilaterally leaked out of the leakage path in all foam models during the injection of the fourth blue cement portion with one exception (specimen S3 with no cement leakage, as shown in Figure 4C).

Mean total lengths of each cement portion are shown over the 36 beams in a stacked radar diagram in Figure 5. Respective SDs of the total lengths are similarly shown in Figures 6A–6D for each cement portion separately. Mean distances to border of the whole cement unit together with their respective SDs are shown in Figure 7 by means of a radar diagram.

Table 1 presents the two highest values for mean total lengths of each cement portion and mean distances to border of the whole cement unit, both rated among all 36 beam directions, with designation of associated SDs and beam directions. The two highest values for the first three injection steps and the total cement unit were found in directions anterior bilateral to the cannula along the 120°, 240° and 250° beams with one exception in direction posterolateral to the cannula along the 60° beam. The two highest values for the fourth injection step were registered in the direction of the cannula along the 170° and 180° beams.

Table 2 shows the two highest values for SDs of total lengths and distances to border, rated among the 36 beam directions under consideration of all specimens, with designation of associated beam directions. The two highest values were found anterior bilateral to the cannula along the 120°, 150°, 240° and 250° beams for the last three injection steps and the total cement unit with one exception in direction opposite to the direction of the cannula along the 10° beam. The two highest values for the first injection step were registered posterior bilateral to the cannula along the 70° and 350° beams.

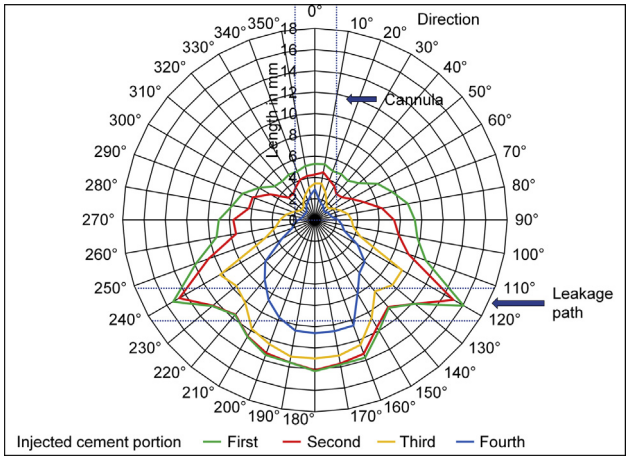

Figure 5 Total length values shown in terms of stacked mean values over the 36 beams. Starting from the fourth cement portion, the values of all previously injected portions were added to the subsequently injected ones and assigned to the respective colour. In accordance to the observed distribution pattern, the values for the firstly injected portions are distributed at the outer border.

Averaged SDs of total lengths and distances to border under consideration of all 36 beam directions are presented in Table 3. Their values related to the fourth cement portion (total lengths) and the whole cement amount (distances to border) were significantly higher in comparison to the first cement portion ($p \leq 0.020$). No further significant differences were detected in this respect.

The fourth cement portion was with the biggest surface area, averaged among all specimens, followed by the third, second and first cement portions (Table 3). All comparisons between the pairs of cement portions revealed significant differences ($p < 0.001$) with one exception between the second and third portions.

The intersection volume, calculated from the CT scans, was 1.74 mL, corresponding to 47% from the totally injected cement amount in each specimen.

The dynamic cement viscosity measured 180 seconds after the start of polymerization was 343 ± 108 Pa·s and increased to 659 ± 208 Pa·s after 330 seconds.

Discussion

The aim of the present study was to investigate bone cement distribution in artificial inhomogeneous cancellous bone structures under a stepwise injection procedure.

The analysis of the specimens' cross sections indicates that the cement inflated inside-out, with the previously injected cement portion being pushed outwards in all directions by the subsequently injected one. The assumption of inside-out cement inflation is supported by the fact that the calculated surface area increased from the first to the last injected portion. Apart from diffuse transitions between the cement portions, this push-out process resulted in no cement intermixture. The nonmixing behaviour can be ascribed to the injection parameters, favoring a predominantly creeping cement flow. Creeping flow is characterised as a flow with viscous forces dominating over dynamic forces [19], as it is the case with highly viscous materials and/or slow flow velocities. Intermixing of different cement portions underlying creeping flow is practically impossible [20,21]. Despite the fact that the different cement portions did not intermix, the transitions at the interface between them were diffuse, assuming that an interdigitation amongst the cement portions takes place. As a result, the portions would then ideally be merged into one mechanical cement unit, which is being inflated in the course of injection steps. However, the mechanical properties of this unit need to be investigated yet.

With regard to the directional flow analysis, the main finding was that the individual cement portions preferably flow with the most inhomogeneous cement distribution inside the leakage path. The leakage path can, therefore, be considered as the most important adverse injection parameter, preventing a more homogeneous cement distribution. The second adverse injection parameter was most likely the existing simulated bone marrow, which seemed to have enhanced a rather inhomogeneous cement distribution in directions different than the ones of the leakage path. Based on this, some elevated dispersion was

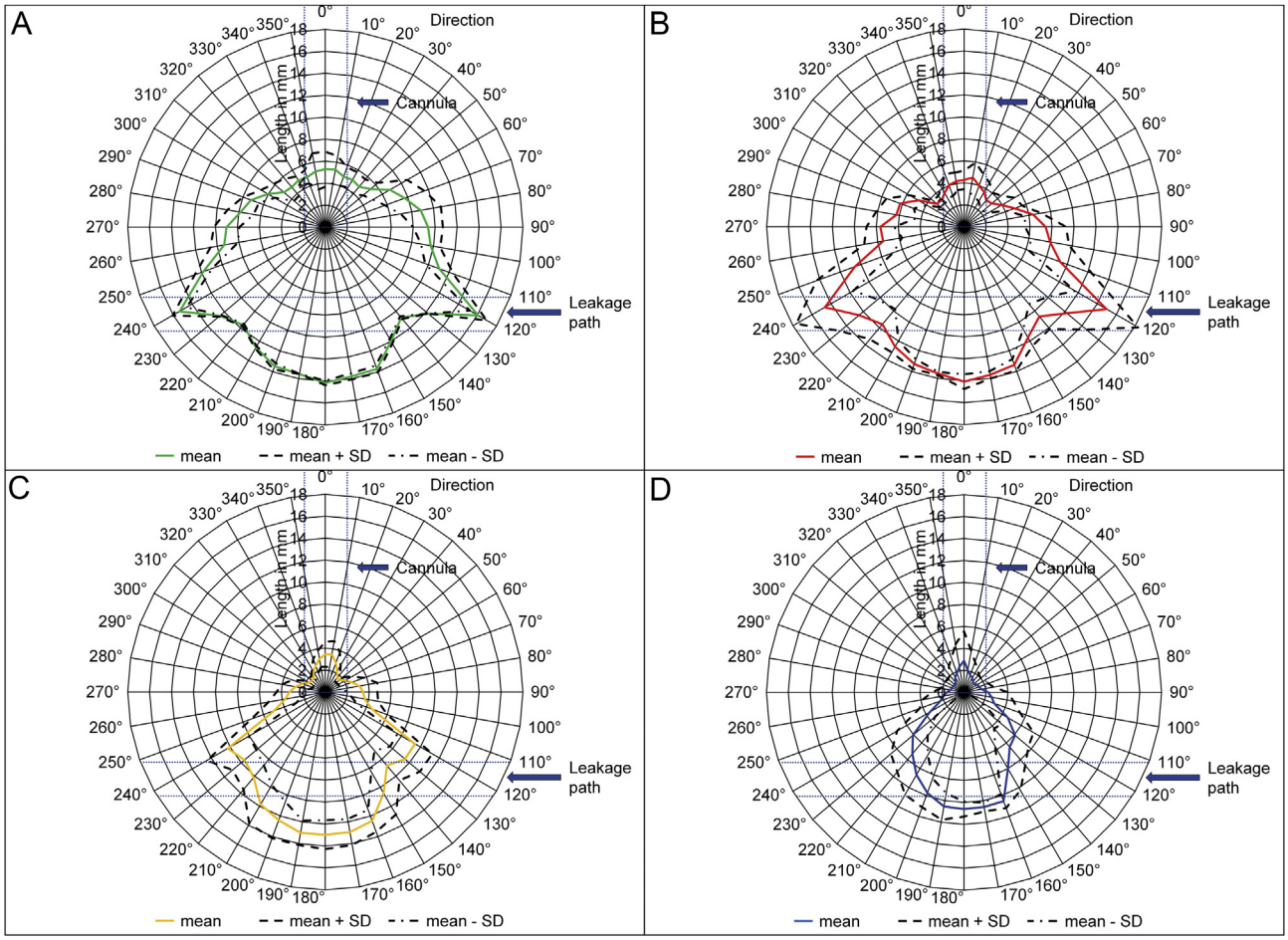

Figure 6 Total length values shown in terms of stacked mean and standard deviation values over the 36 beams for each cement portion separately. Starting from the fourth cement portion, the values of all previously injected portions were added to the subsequently injected ones and assigned to the respective colour. Based on these, respective standard deviations were added to each cement portion. (A) First cement portion; (B) second cement portion; (C) third cement portion; (D) fourth cement portion.

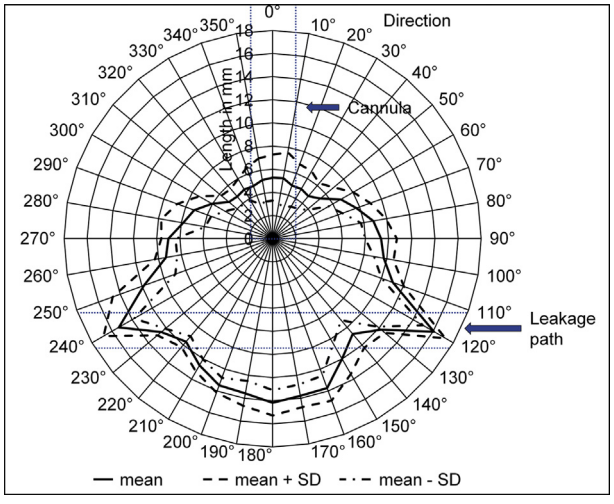

Figure 7 Distance to border values shown in terms of mean and standard deviation values over the 36 beams. Mean values are identical to the stacked values of the firstly injected cement portion.

observed in posterolateral direction, opposite to the direction of injection. In a previous study by Bohner et al [22], it has been evidenced that models similar to the ones used in the current study, featuring a large diameter hole filled with high-viscosity bone marrow substitute, provoke uneven cement distribution and cement leakage. A more spherical and thus less dispersed expansion (with smaller deviations) would take place if the cement had been injected into a geometrically more homogeneous model, i.e., with no leakage path and no bone marrow.

Clinically, cement leakage has been shown to occur most commonly at the basivertebral and external vertebral venous plexus [23], which is based on the anatomy and orientation of the basivertebral veins within the vertebral body and their communication with the anterior external vertebral plexuses at the anterolateral sides of the vertebral bodies. The anatomy and orientation of these potential leakage paths varies from vertebra to vertebra and is, therefore, patient-specific. In order to give a generalised statement about cement leakage, the current study used models which contained one simplified leakage path located at their anterior half and passing perpendicular to the injection direction, with bilateral exit points.

Table 1 The two highest values for mean total lengths of each cement portion and mean distances to border of the total cement unit as rated among all 36 beam directions, with designation of associated standard deviations and beam directions.

Injected cement	Parameter	
	Total length (mm)	Beam direction (°)
First portion	2.84 ± 1.80	60
	1.85 ± 1.27	260
Second portion	5.55 ± 3.32	120
	5.62 ± 3.72	250
Third portion	4.81 ± 1.83	120
	6.62 ± 2.20	240
Fourth portion	10.58 ± 0.41	170
	10.62 ± 0.68	180
	Distance to border (mm)	
Total unit	16.08 ± 1.14	120
	15.32 ± 1.52	240

Table 2 The two highest values for standard deviations (SD) of total lengths of each cement portion and distances to border of the total cement unit as rated among all 36 beam directions under consideration of all specimens, with designation of associated beam directions.

Injected cement	SD (mm)	Beam direction (°)
First portion	1.92	70
	1.68	350
Second portion	3.32	120
	3.72	250
Third portion	2.25	150
	2.20	240
Fourth portion	2.70	120
	3.40	240
Total unit	2.27	10
	2.88	250

Regardless of the abovementioned findings and under consideration of the totally injected cement as one unit, the distances from the centre of the circular section to the outer cement border deviated moderately from their mean value, which confirms the fulfillment of requirements for a rather uniform cement distribution. In addition, the two-dimensional spatial distribution of those distances amongst the 36 beams directions was more homogeneous in comparison to the parameters characterising the four individual cement portions. Therefore, the existence of a leakage path does not seem to considerably affect the homogeneity of the distribution of the totally injected cement unit. This can be accredited to the rheological properties of the used cement. The viscosity measured 180 and 330 s after cement mixing highlights its ready-to-use characteristics with a medium viscosity immediately after mixing. Other cements, such as the one used in the study by Baroud et al [10], have a significantly lower initial viscosity and require a remarkable waiting time of at least 10 minutes until the viscosity reaches 270 Pa·s, upon which uniform filling can be expected. The viscosity in the present study increased twofold within the time period between the start of the first and the end of the last injection and was slightly higher in comparison to the measurements performed by Deusser et al [15] with the same cement composition. The differences could have arisen from different mixing procedures. Nevertheless, the progression of increasing viscosity showed the same tendency in both studies.

The calculated intersection volume of 1.74 mL was relatively small and does not fully support the statement of homogeneous cement distribution. However, considering the relatively high bone marrow viscosity, as well as the leakage path and the porous foam structure itself, the injection parameters for a homogeneous cement distribution were not ideal, and hence, this result is not surprising.

From a clinical point of view, to achieve a more homogeneous cement distribution, lavage technique is suggested to wash out the bone marrow [11,12], allowing the use of more viscous bone cement, which has been shown to distribute more uniformly [10]. Moreover, it was reported that the uniformity of cement distribution is reduced when the bone marrow viscosity increases [22]. The findings of this work did not reveal any disagreement with previous reports, except the fact that the stepwise injecting procedure is not necessarily capable of preventing cement from leaking, which is a contradictory finding to the generally accepted opinion [10]. However, the time interval between the consecutive injections was approximately 45 s, which was not long enough to let the cement of the first injection polymerise and block the leakage path. A considerably longer waiting time between the first and second injections would have made this possible.

A major limitation of the present study was the manual cement mixing procedure, which resulted in cumulated air enclosures in each cement portion that affected the results, especially the CT image processing. This manual procedure was chosen as it allowed uniform preparation of each bone cement portion with the same start point of curing. Another limitation was the immolation of the physiological environment by using foam models as substitutes for human vertebrae, together with cast resin outer shell, mimicking cortical bone, and intertrabecular pores filled with a water—cornstarch mixture, mimicking bone marrow. However, each of the components was selected to resemble a human vertebra as close as possible. Moreover,

Table 3 Averaged standard deviations (SD) of total lengths of each cement portion and distances to border of the total cement unit under consideration of all 36 beam directions, together with the surface area mean and standard deviation values among all specimens.

Injected cement	Averaged SD (mm)	Surface area (mm^2)
First portion	0.83	54.7 ± 12.5
Second portion	1.33	98.9 ± 7.4
Third portion	1.12	108.9 ± 10.3
Fourth portion	1.53	141.6 ± 11.2
Total unit	1.28	404.2 ± 14.9

the focus of this work was to investigate the characteristics of bone cement behaviour, premising to mimic rather more homogeneous than physiological conditions.

The experimental results obtained in this study could serve to validate future simulations addressing the flow through porous media, such as osteoporotic cancellous bone. Thus, one requirement will be to achieve good compliance between the experimental and computational approach under the consideration of the stepwise injection process.

Conclusion

The simulated leakage path seemed to be the most important adverse injection factor influencing the homogeneity of the cement distribution. Another adverse factor causing dispersion of this distribution was represented by the simulated bone marrow. However, considering all four cement portions together, the rather uniform distribution of the totally injected cement as one unit could be ascribed to the use of medium-viscous cement and its ability to generate relatively uniform filling pattern. Finally, with its short waiting time of 45 s, the stepwise injection procedure was shown to be ineffective in terms of preventing cement leakage.

Conflicts of Interest

The authors are not compensated, and there are no other institutional subsidies, corporate affiliations or funding sources supporting this work unless clearly documented and disclosed.

Funding/Support

This investigation was performed with the assistance of the AO Foundation.

Acknowledgements

The authors kindly thank the coworkers Mauro Bluvol and Sandra Thöny from the AO Research Institute Davos, Switzerland, for their support in data evaluation.

References

[1] Wong CC, McGirt MJ. Vertebral compression fractures: a review of current management and multimodal therapy. J Multidiscip Healthc 2013;6:205—14.
[2] Heini PF, Walchli B, Berlemann U. Percutaneous transpedicular vertebroplasty with PMMA: operative technique and early results. A prospective study for the treatment of osteoporotic compression fractures. Eur Spine J 2000;9:445—50.
[3] Mathis JM, Barr JD, Belkoff SM, Barr MS, Jensen ME, Deramond H. Percutaneous vertebroplasty: a developing standard of care for vertebral compression fractures. AJNR Am J Neuroradiol 2001;22:373—81.
[4] Deramond H, Mathis JM. Vertebroplasty in osteoporosis. Semin Musculoskelet Radiol 2002;6:263—8.
[5] Jensen ME, Dion JE. Vertebroplasty relieves osteoporosis pain. Diagn Imaging (San Franc) 1997;19(68):71—2.
[6] Berlemann U, Ferguson SJ, Nolte LP, Heini PF. Adjacent vertebral failure after vertebroplasty. A biomechanical investigation. J Bone Joint Surg Br 2002;84:748—52.
[7] Baroud G, Bohner M. Biomechanical impact of vertebroplasty. Postoperative biomechanics of vertebroplasty. Joint Bone Spine 2006;73:144—50.
[8] Rauschmann MA, Von Stechow D, Thomann KD, Scale D. Complications of vertebroplasty. Der Orthopäde 2004;33:40—7.
[9] Do HM. Intraosseous venography during percutaneous vertebroplasty: is it needed? AJNR Am J Neuroradiol 2002;23:508—9.
[10] Baroud G, Crookshank M, Bohner M. High-viscosity cement significantly enhances uniformity of cement filling in vertebroplasty: an experimental model and study on cement leakage. Spine (Phila Pa 1976) 2006;31:2562—8.
[11] Boger A, Benneker LM, Krebs J, Boner V, Heini PF, Gisep A. The effect of pulsed jet lavage in vertebroplasty on injection forces of PMMA bone cement: an animal study. Eur Spine J 2009;18:1957—62.
[12] Benneker LM, Heini PF, Suhm N, Gisep A. The effect of pulsed jet lavage in vertebroplasty on injection forces of PMMA bone cement, material distribution and potential fat embolism; a cadaver study. Spine 2008;33:E906—10.
[13] Boger A, Wheeler K. A medium viscous acrylic cement enhances uniformity of cement filling and reduces leakage in cancellous bone augmentation. ISRN Materials Science 2011; 2011. 7 pages.
[14] Heini PF, Dain Allred C. The use of a side-opening injection cannula in vertebroplasty: a technical note. Spine (Phila Pa 1976) 2002;27:105—9.
[15] Deusser S, Sattig C, Boger A. Rheological and curing behavior of a newly developed, medium viscous acrylic bone cement. ISRN Mater Sci 2011;2011:8.
[16] Gisep A, Boger A. Injection biomechanics of in vitro simulated vertebroplasty - correlation of injection force and cement viscosity. Biomed Mater Eng 2009;19:415—20.
[17] Basafa E, Murphy RJ, Kutzer MD, Otake Y, Armand M. A particle model for prediction of cement infiltration of cancellous bone in osteoporotic bone augmentation. PLoS One 2013;8: e67958.
[18] Bleiler C, Wagner A, Stadelmann VA, Windolf M, Kostler H, Boger A, et al. Multiphasic modelling of bone-cement injection into vertebral cancellous bone. Int J Numer Method Biomed Eng 2015;31(1):e02696.
[19] Kirby BJ. Micro-and nanoscale fluid mechanics: transport in microfluidic devices. Cambridge University Press; 2010.
[20] Aref H. Stirring by chaotic advection. J fluid Mech 1984;143:1—21.
[21] Wang G, Yang F, Zhao W. There can be turbulence in microfluidics at low Reynolds number. Lab Chip 2014;14:1452—8.
[22] Bohner M, Gasser B, Baroud G, Heini P. Theoretical and experimental model to describe the injection of a polymethylmethacrylate cement into a porous structure. Biomaterials 2003;24:2721—30.
[23] Yeom JS, Kim WJ, Choy WS, Lee CK, Chang BS, Kang JW. Leakage of cement in percutaneous transpedicular vertebroplasty for painful osteoporotic compression fractures. J Bone Joint Surg Br 2003;85:83—9.